Three-dimensional photodissociation in strong laser fields: Memory-kernel effective-mode expansion

Xuan Li,[1,*] Ioannis Thanopulos,[2,†] and Moshe Shapiro[1,3,‡]

[1]*Department of Chemistry, The University of British Columbia, Vancouver, British Columbia V6T 1Z3, Canada*

[2]*Theoretical and Physical Chemistry Institute, National Hellenic Research Foundation, Athens 11635, Greece*

[3]*Department of Chemical Physics, The Weizmann Institute, Rehovot 76100, Israel*

(Received 16 July 2010; revised manuscript received 17 January 2011; published 21 March 2011)

We introduce a method for the efficient computation of non-Markovian quantum dynamics for strong (and time-dependent) system-bath interactions. The past history of the system dynamics is incorporated by expanding the memory kernel in exponential functions thereby transforming in an exact fashion the non-Markovian integrodifferential equations into a (larger) set of "effective modes" differential equations (EMDE). We have devised a method which easily diagonalizes the EMDE, thereby allowing for the efficient construction of an adiabatic basis and the fast propagation of the EMDE in time. We have applied this method to three-dimensional photodissociation of the H_2^+ molecule by strong laser fields. Our calculations properly include resonance-Raman scattering via the continuum, resulting in extensive rotational and vibrational excitations. The calculated final kinetic and angular distribution of the photofragments are in overall excellent agreement with experiments, both when transform-limited pulses and when chirped pulses are used.

DOI: 10.1103/PhysRevA.83.033415 PACS number(s): 33.80.Gj, 03.65.−w

I. INTRODUCTION

One of the most important and challenging problems in physics and chemistry is the proper treatment of the quantum dynamics of a *system*, consisting of a small number of states, coupled to a *bath*, consisting of a very large number, often infinite, number of states [1]. The difficulty is most pronounced when the system-bath interaction is strong and time dependent, e.g., when intense external (laser) fields are involved. One would like to develop methods that incorporate the mutual system-bath effects in an exact, yet computationally efficient, way.

The photophysics of molecules in intense electromagnetic fields, which is a prototype of strong time-dependent system-bath interaction, has been widely investigated [2], mostly in relatively small molecules [3–5]. In particular, the rapid development of ultrafast strong-field photodissociation (PD) and ionization processes has attracted great attention [6–11]. It has been shown that the strong interaction of matter with femto- and attosecond pulses depends very sensitively on laser peak intensity, carrier envelope phase, and pulse duration. The studies of the simplest molecules, H_2 and H_2^+, have enhanced our understanding of the dynamics and control of strong-field dissociation processes in other (possibly polyatomic) molecules.

Over the years a number of methods, such as wave packet propagation on a grid, which directly solve the time dependent Schrödinger equation, sometimes in conjunction with Floquet-type expansions [12] have been developed for the study of strong-field photodissociation. Due to numerical difficulties of applying such methods in full three-dimensional space, especially when long propagation times (such as in the present case) are involved, these methods are limited to situations involving only a relatively small number of bound states and continuum channels. The inclusion of the highly important (and numerous) continuum rotational channels which get excited by the strong laser pulse becomes prohibitively expensive.

In this study we introduce a theoretical approach which enables us to perform strong-field molecular PD calculations involving large numbers of bound states and continuum channels with high efficiency. The computational ease is a result of expressing the problem in terms of a large set of "effective-modes" differential equations (EMDE) [13] and diagonalizing these equations in an essentially analytical manner. We demonstrate this procedure by performing a full three-dimensional computation on the H_2^+ PD by strong near-IR femtosecond laser pulses.

II. THEORY

As depicted schematically in Fig. 1, we consider the strong interaction of a system, composed of bound states, with a bath, composed of continuum states, mediated by an external laser field. The total Hamiltonian is given as $H = H_M + H_{int}$, where H_M is the radiation-free system and the bath material Hamiltonian; and $H_{int} = -\vec{\mu}\cdot\vec{\epsilon}$ is the system-bath radiation-matter interaction term, with $\vec{\epsilon}$ and $\vec{\mu}$ denoting, respectively, the classical electric field and the electric dipole operator. Using the bound ("system"), $|E_i\rangle$,$(i = 1,\ldots,N_b)$, and continuum ("bath"), $|E,n^-\rangle$, eigenstates of H_M, obeying the $[H_M - E_i]|E_i\rangle = [H_M - E]|E,n^-\rangle = 0$ eigenvalue equations, we expand $|\Psi\rangle$, the solution of the total, $i\hbar\partial|\Psi\rangle/\partial t = H|\Psi\rangle$, system-bath Schrödinger equation as

$$|\Psi(t)\rangle = \sum_{i=1}^{N_b} b_i|E_i\rangle + \sum_n \int dE b_{E,n} e^{-iEt}|E,n^-\rangle. \quad (1)$$

By substituting Eq. (1) into the time-dependent Schrödinger equation and using atomic units ($\hbar = 1$), we obtain two sets of

*xli3536@chem.ubc.ca
†ithano@eie.gr
‡mshapiro@chem.ubc.ca

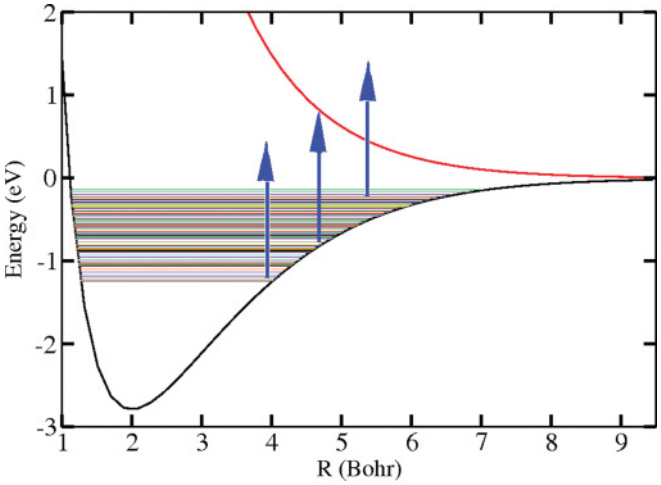

FIG. 1. (Color online) A schematic plot of the photodissociation of H_2^+ due to the $1s\sigma_g \rightarrow 2p\sigma_u$ transition.

coupled equations:

$$\dot{b}_E = i\sum_{j=1}^{N_b} \mu(E,n;j)\varepsilon(t)e^{iEt}b_j(t), \tag{2}$$

$$\dot{b}_i = -iE_i b_i + i\sum_n \mu(i;E,n)b_{E,n}\varepsilon(t)e^{-iEt}. \tag{3}$$

with $\mu(E,n;j) \equiv \langle E,n^-|\mu_k|E_i\rangle$ standing for the bound-continuum dipole matrix elements. Integrating Eq. (2)

$$b_{E,n}(t) = i\int_{-\infty}^{t} dt' \sum_{j=1}^{N_b} \mu(E,n;j)b_j(t')\varepsilon(t')e^{iEt'}, \tag{4}$$

and substituting into Eq. (3) leads to a set of integrodifferential equations (IDE)

$$\dot{b}_i = -iE_i b_i + i\sum_{j=1}^{N_b}\int_{-\infty}^{t} dt' b_j(t')F_{i,j}(t-t')\varepsilon(t)\varepsilon(t'). \tag{5}$$

In the above, $F_{i,j}$ are *cross-correlation* functions defined as

$$F_{i,j}(\tau) = i\int dE \sum_n \mu(i;E,n)\mu(E,n;j)e^{-iE\tau}, \tag{6}$$

which serve as "memory-kernels." The Markovian approximation, $F_{i,j}(t-t') \approx F_{i,j}(t)\delta(t-t')$, can be made when the field is weak or narrow in energy bandwidth, neither of which is applicable for strong field-matter interaction of femtosecond duration. Nevertheless, the solution of Eq. (5) can be greatly simplified if the memory kernels can be written in a separable form as $F_{i,j}(t-t') = f_{i,j}(t)g_{i,j}(t')$. Therefore, each cross-correlation function is fitted to the desired accuracy within the time interval of interest (see also Ref. [14] on this issue), as a sum of N_c exponential functions

$$F_{i,j}(\tau) = \sum_{s=1}^{N_c} Z_{i,j}^{(s)} \exp(-i\Omega^{(s)}\tau - \Gamma|\tau|), \tag{7}$$

where $Z_{i,j}^{(s)}$ are, in general, complex parameters, and $\Omega^{(s)}$ and Γ are real.

We now define the "effective mode" variable $c_{s,i}$ as

$$c_{s,i}(t) = \sum_{j=1}^{N_b}\int_{-\infty}^{t} dt' b_j(t')Z_{i,j}^{(s)}e^{i\Omega^{(s)}t'}e^{-\Gamma(t-t')}\varepsilon(t'), \tag{8}$$

and write Eq. (5) as

$$\dot{b}_i(t) = -iE_i b_i(t) + i\varepsilon(t)\sum_{s=1}^{N_c} e^{-i\Omega^{(s)}t}c_{s,i}(t). \tag{9}$$

The first derivative of $c_{s,i}$ is then

$$\dot{c}_{s,i}(t) = -\Gamma c_{s,i}(t) + \sum_{j=1}^{N_b} b_j(t)Z_{i,j}^{(s)}e^{i\Omega^{(s)}t}\varepsilon(t). \tag{10}$$

We now define a new vectorial basis set $\underline{\mathbf{d}} = (\underline{\mathbf{b}},\underline{\mathbf{c}})$ and rewrite the Eqs. (9) and (10) as "effective modes" differential equations (EMDE),

$$\dot{\underline{\mathbf{d}}} = \underline{\underline{\mathbf{h}}}\cdot\underline{\mathbf{d}}, \text{ with } \underline{\underline{\mathbf{h}}} = \begin{bmatrix} \underline{\underline{\mathbf{h}}}^{\mathbf{bb}} & \underline{\underline{\mathbf{h}}}^{\mathbf{bc}} \\ \underline{\underline{\mathbf{h}}}^{\mathbf{cb}} & \underline{\underline{\mathbf{h}}}^{\mathbf{cc}} \end{bmatrix}, \tag{11}$$

where $\underline{\underline{\mathbf{h}}}$ is a general complex square matrix of rank $N_b(N_c+1)$, with $\underline{\underline{\mathbf{h}}}^{\mathbf{bb}}$ and $\underline{\underline{\mathbf{h}}}^{\mathbf{cc}}$ being diagonal square submatrices of rank N_b and N_bN_c, respectively. These four sub-blocks are defined by

$$[\mathbf{h}^{bb}]_{ij} = -i\frac{E_i}{\hbar}\delta_{ij}, \tag{12}$$

$$[\mathbf{h}^{bc}]_{ij} = \delta_{ik}\frac{i}{\hbar}\varepsilon(t)\exp(-i\Omega^{(s)}t) \equiv \delta_{ik}f_s(t) \tag{13}$$

with

$$\begin{aligned} k &= (j-N_b-1)/N_s+1, \\ s &= j-N_b-(k-1)N_s, \end{aligned} \tag{14}$$

and

$$[\mathbf{h}^{cb}]_{ij} = Z_{k,j}^{(s)}\exp(i\Omega^{(s)}t)\varepsilon(t) \equiv g_{k,j}^{s}(t)\varepsilon(t) \tag{15}$$

with

$$\begin{aligned} k &= (i-N_b-1)/N_s+1, \\ s &= i-N_b-(k-1)N_s, \end{aligned} \tag{16}$$

and

$$[\mathbf{h}^{cc}]_{ij} = -\Gamma\delta_{i,j}. \tag{17}$$

This effective, in general complex, Hamiltonian is neither Hermitian nor symmetric.

Defining $\underline{\underline{\mathbf{U}}}$, the matrix of eigenvectors of $\underline{\underline{\mathbf{h}}}$, namely,

$$\underline{\underline{\mathbf{U}}}\cdot\underline{\underline{\mathbf{h}}} = \hat{\underline{\underline{\lambda}}}\cdot\underline{\underline{\mathbf{U}}}, \tag{18}$$

with $\hat{\underline{\underline{\lambda}}}$ being the diagonal matrix of eigenvalues, allows us to define a basis of dressed states $\underline{\mathbf{f}} = \underline{\underline{\mathbf{U}}}\cdot\underline{\mathbf{d}}$. It is convenient to integrate Eq. (11) using the *adiabatic* basis over a number of segments in t. Within each small segment we approximate $\underline{\underline{\mathbf{U}}}$ as constant and thus the *nonadiabatic* coupling is zero; in the boundaries between different segments we transform back to the bare basis in order to assure continuity of the solutions

in the bare basis and then transform to a new *adiabatic* basis for the next segment so that the nonadiabatic couplings and curve crossings are explicitly taken care of. This integration technique is akin to the "piecewise" method for solving quantum close-coupling equations [15], and numerical study shows a 0.5% relative error in the final results by using the adiabatic basis. Note, however, that use of the adiabatic basis should be always checked with respect to the integration time step $\Delta t \equiv [t_k - t_{k-1}]$. For a sufficiently small Δt, and defining

$$\underline{\underline{\hat{\mathbf{W}}}}(t_{k+1},t_k) = \exp \int_{t_k}^{t_{k+1}} \underline{\underline{\hat{\lambda}}}(t)\, dt, \tag{19}$$

we can propagate the $\underline{\mathbf{d}}$ vector,

$$\underline{\mathbf{d}}(t_{k+1}) = \underline{\underline{\mathbf{U}}}^{-1}(t_{k+1}) \cdot \underline{\underline{\hat{\mathbf{W}}}}(t_{k+1},t_k) \cdot \underline{\underline{\mathbf{U}}}(t_k) \cdot \underline{\mathbf{d}}(t_k). \tag{20}$$

The crucial development for this work is that we have found an analytical way of computing the $\lambda_i(t)$ eigenvalues. It is possible to show (see Appendix A) that there are $N_b(N_c - 1)$ "dark" eigenvalues, $\lambda_i = -\Gamma$, and a much smaller number, $M = 2N_b$, of "bright" eigenvalues, computed by diagonalizing an $M \times M$ matrix. The term "bright" ("dark") eigenvalues is related to the fact that the corresponding eigenvectors are coupled (uncoupled) to the initial "real" bound states. Note, we construct the $\underline{\underline{\mathbf{U}}}$ matrix analytically so that self-orthogonality is explicitly satisfied (see Appendix B), and we further exploit that $\underline{\underline{\mathbf{U}}}(t_k) \cdot \underline{\underline{\mathbf{U}}}^{-1}(t_{k+1}) \approx \underline{\underline{\mathbf{1}}}$, which is valid for sufficiently small Δt.

As a result of the above simplifications the effort associated with the numerical propagation of Eq. (20) is drastically reduced. For example, for the strong-field PD of the H_2^+ presented below, we consider $N_b = 91$ system (bound) states (seven vibrational manifolds of 13 rotational states each), and $N_c = 77$ effective modes. The time propagation requires the eigenvalues and eigenvectors of the matrix $\underline{\underline{\mathbf{h}}}$ of rank ≈ 7000 for each one of the 5000 time steps. This calculation was performed on a *single* Intel Xeon EMT64 processor in about 1 CPU hour, for each pulse configuration, and the required memory was less than 250 Megabyte.

III. RESULTS

We now present our results for the near-IR strong field PD of H_2^+, depicted schematically in Fig. 1. In these computations we have assumed that the initial vibrational distribution of H_2^+ is given by the Frank-Condon overlap integrals with the ground state H_2 parent molecule, with the rotational distribution being determined by the temperature of the H_2 gas in the ion source [16]. We have confirmed the validity of these initial conditions by performing a weak-field PD calculation and verifying that its kinetic energy release (KER) distributions are in excellent agreement with experiments [17].

In Fig. 2, we present the time dependence of various bound and continuum ro-vibrational states during and after the action of a 120 fs transform-limited $I_{\rm peak} = 5 \times 10^{12}$ W/cm^2 pulse on the $V_b = 7$, $J_b = 0$ initial state of H_2^+. The degree of rotational excitation during the pulse of both the bound and continuum manifolds displayed here is by far more extensive than that expected on the basis of perturbation theory, indicating strong bound-continuum Rabi flopping prior to dissociation.

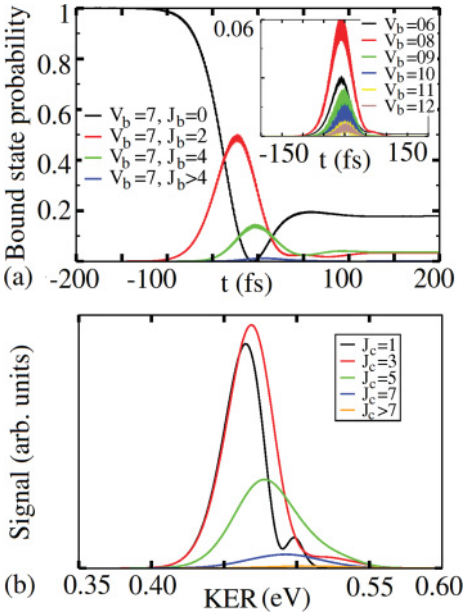

FIG. 2. (Color online) Calculated: (a) time-dependent rovibrational states probabilities with initially populated $V_b = 7$, $J_b = 0$; small inset for other transiently populated vibrational bands. (b) Final KER spectra for different rotational states.

In addition, we find remnants of the $V_b = 7$, $J_b = 2,4$ ro-vibrational states after the pulse is gone, with the post-pulse probabilities of both rotational states amounting to 4%–5%. The induced rotational Raman pumping in the ground state of H_2^+ has been shown to occur for other systems [18], too. Some vibrational redistribution also occurs, as shown in the inset of Fig. 2(a), making it clear why an extensive rovibrational basis had to be used in the calculation. In Fig. 2(b), the final KER spectra of the photofragments for different rotational states are shown, displaying extensive rotational excitation of continuum channels.

We now present calculations of the angular distribution of the (proton and H atom) photofragments. Our results are three dimensional, since the rovibrational states used depend on the internuclear distance, and the two angular coordinates of the linear H_2^+ molecule. However, for a linearly polarized pulse, the dynamics with respect to the m quantum number is separable, thus effectively resulting into equations describing two-dimensional dynamics. Such a calculation, involving an extensive excitation of rotational channels by an intense pulse lasting relatively long times (~100 fs), is significantly more efficient within our methodology, for the reasons discussed above, than other methods which have been used to attack the problem of photodissociation of H_2^+ in strong laser fields. The top panel of Fig. 3 shows a contour plot of the computed angular probability distribution as a function of the KER and $\cos\theta$, where θ is the polar angle of the fragments' motion relative to the laser polarization. The computation is performed for a 120 fs transform-limited pulse with $I_{\rm peak} = 3 \times 10^{12}$ W/cm^2. Two main features are worth noticing: 1) the alignment of the photofragments near the $\theta = 0, \pi$ points, and 2) the dominance of the 0.68 eV KER peak (due to PD from the $V_b = 8$ manifold) and that of the 0.84 eV KER

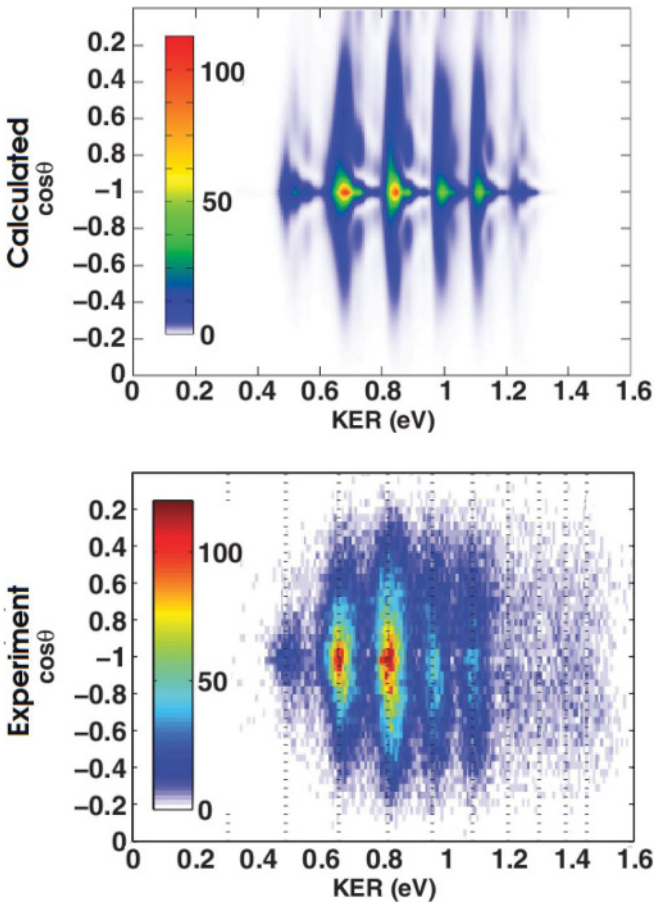

FIG. 3. (Color online) The angular distribution (relative to the polarization direction) of the $H + H^+$ photofragments as a function of their kinetic energy release by a transform-limited pulse with peak intensity ($I_{\text{peak}} = 3 \times 10^{12}$ W/cm^2). Computed: top panel; experiment (taken from Ref. [17]): bottom panel.

peak (due to PD from the $V_b = 9$ manifold). The prominent PD from the $V_b = 8$ manifold is definitely a non-Markovian strong field effect; we have calculated (not shown here) that a Markovian and a non-Markovian calculation differ by 40 meV in KER, 18% in signal strength, and 50% in signal width, at the excitation parameters corresponding to Fig. 3. The computed results are contrasted with the experiment of Prabhudesai *et al.* [17] (Fig. 3 lower panel). The computed degree of alignment and KER distribution agree very well with the experiment. The fact that the experimental distribution is slightly more spread out is mainly due to some (as yet) experimental uncertainty in the initial temperature of the H_2^+ molecular ion.

We have also studied the effect of pulse-shape by applying to a 30 fs pulse a quadratic phase chirp whose group delay dispersion is 630 fs^2, thereby stretching the pulse duration to 120 fs. The dominant rovibrational state in this PD process by a 795 nm laser is the $V_b = 9$, J_b state (states with $J_b = 3$ are most populated in the initial ion source). In Fig. 4, we show the KER spectra for a negatively chirped pulse, at different I_{peak} for initially populated $V_b = 9$, $J_b = 3$ state. According to Fig. 4 the major dissociation peak in the KER spectra shifts to higher energies with a negatively chirp pulse for the initially populated $V_b = 9$, $J_b = 3$ state as the laser intensity

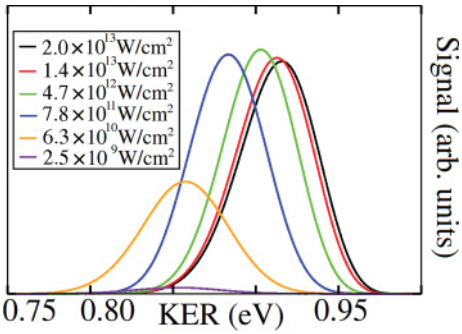

FIG. 4. (Color online) KER spectra of H_2^+ for negatively chirped pulse taken at different peak intensities for an initial state of $V_b = 9$, $J_b = 3$.

increases; this effect is in complete agreement with the results in Ref. [17].

IV. CONCLUSION

In conclusion, we have presented an efficient approach for non-Markovian quantum-dynamics of strong (and time-dependent) system-bath couplings. The method uses the expansion of the memory kernels in effective modes and the essentially analytic diagonalization of the resulting propagation equations. Importantly, the method is singled out in that it can also directly use the results from experimental methods capable of revealing the amplitude and phase of molecular spectra [19]; its reliance on computed memory kernels, which can be problematic, is thus minimized. Our method is also proved useful in modeling Feshbach and/or shape resonances of scattering states in a photo-associating process (time reversal of PD) [20]. We have applied this method to the strong-field PD of H_2^+, where, due to Raman scattering via the continuum, the inclusion of numerous rovibrational states is necessary for the understanding of the final photofragments' angular distributions and their correlation with the KER spectra. Future work on non-Markovian dynamics of large systems with other coupling schemes than presented here are planned.

ACKNOWLEDGMENTS

We wish to thank V. Milner and E. Shapiro for discussions and V. Prabhudesai, U. Lev, A. Natan, and Y. Silberberg for communicating and clarifying to us their experimental results. This work was supported by a "Major Thematic Grant" of the Peter Wall Institute for Advanced Studies of the University of British Columbia; by NSERC Discovery Grant; and by the US DoD DTRA program. I.T. acknowledges financial support from the EU-FP7 program under Grant Agreement No. PIRG03-GA-2008-230943 (COPET).

APPENDIX A: OBTAINING THE EIGENVALUES OF h

Our diagonalization scheme is based on the fact that the particular structure of $\mathbf{h}$ of Eq. (11) guarantees that it is related by a similarity transformation to a block-diagonal matrix of the form

$$\mathbf{h}' = \begin{bmatrix} \mathbf{h}_P & \mathbf{0} \\ \mathbf{0} & \mathbf{h}_{EM} \end{bmatrix}, \tag{A1}$$

where the first, "physical" (P), block is of size M by M and the second, "Effective-Modes" (EM), block is given as $-\Gamma \cdot \mathbf{I}$, where $\mathbf{I}$ is an $N_b \times (N_s - 1)$ by $N_b \times (N_s - 1)$ unit matrix. The physical block can be expressed as

$$\mathbf{h}_P = \begin{bmatrix} A_1 & 0 & \dots & 0 & 1 & 0 & \dots & 0 \\ 0 & A_2 & \dots & 0 & 0 & 1 & \dots & 0 \\ \dots & \dots & \dots & \dots & \dots & \dots & \dots & \dots \\ 0 & 0 & \dots & A_{N_b} & 0 & 0 & \dots & 1 \\ \sum_s f_s g^s_{11} & \sum_s f_s g^s_{12} & \dots & \sum_s f_s g^s_{1N_b} & -\Gamma & 0 & \dots & 0 \\ \sum_s f_s g^s_{21} & \sum_s f_s g^s_{22} & \dots & \sum_s f_s g^s_{2N_b} & 0 & -\Gamma & \dots & 0 \\ \dots & \dots & \dots & \dots & \dots & \dots & \dots & \dots \\ \sum_s f_s g^s_{N_b 1} & \sum_s f_s g^s_{N_b 2} & \dots & \sum_s f_s g^s_{N_b N_b} & 0 & 0 & \dots & -\Gamma \end{bmatrix}, \tag{A2}$$

where

$$A_k \equiv -i E_k/\hbar,$$

and the f_s and g^s_{ij} terms are defined according to Eqs. (13) and (15).

Because of the similarity transformation, the eigenvalues of the original $N \times N$ ($N \equiv N_b + N_s \times N_b$) $\mathbf{h}$ matrix can be obtained by diagonalizing the $M \times M$ where $M \equiv 2 \times N_b$ physical matrix $\mathbf{h}_P$, supplemented by $N_b \times (N_s - 1)$ replicas of the *same* eigenvalue $\lambda = -\Gamma$. For small N_b and N_s values, it is possible to obtain the similarity transformation matrix between $\mathbf{h}$ and $\mathbf{h}'$ in an analytic fashion using MATHEMATICA. However, as discussed below (Appendix B), the explicit construction of this matrix is not necessary because one can obtain the diagonalizing transformation of the entire $\mathbf{h}$ matrix directly, using the M eigenvectors of $\mathbf{h}_P$.

APPENDIX B: OBTAINING THE EIGENVECTORS OF h

In order to derive the eigenvectors of $\mathbf{h}$, we first arrange its eigenvalues as

$$\lambda = \{\lambda_1, \lambda_2, \dots, \lambda_M, -\Gamma, -\Gamma, \dots, -\Gamma\}. \tag{B1}$$

Due to the particular block-matrix structure of $\mathbf{h}$, the eigenvector matrix $\mathbf{U}$ of Eq. (18) has the following structure:

$$\mathbf{U} = \begin{bmatrix} \mathbf{U}_P \\ \mathbf{U}_{EM} \end{bmatrix} = \begin{bmatrix} U_{1,1} & U_{1,2} & \dots & U_{1,N_b} & U_{1,N_b+1} & \dots & U_{1N} \\ U_{2,1} & U_{2,2} & \dots & U_{2,N_b} & U_{2,N_b+1} & \dots & U_{2N} \\ \dots & \dots & \dots & \dots & \dots & \dots & \dots \\ U_{M,1} & U_{M,2} & \dots & U_{M,N_b} & U_{M,N_b+1} & \dots & U_{MN} \\ 0 & 0 & \dots & 0 & U_{M+1,N_b+1} & \dots & U_{M+1,N} \\ \dots & \dots & \dots & \dots & \dots & \dots & \dots \\ 0 & 0 & \dots & 0 & U_{N,N_b+1} & \dots & U_{N,N} \end{bmatrix}, \tag{B2}$$

where $\mathbf{U}_P$ is of size M by N and $\mathbf{U}_{EM}$ is of size $N_b \times (N_s - 1)$ by N.

We first discuss the analytical construction of $\mathbf{U}_P$. Due to the structure of $\mathbf{h}_P$, it follows from Eq. (18) that the ratios between the elements of the ith row of $\mathbf{U}_P$ satisfy the following equalities:

$$\begin{aligned} U_{i,1} : U_{i,N_b+1} : U_{i,N_b+2} : \dots : U_{i,N_b+N_s} &= (\Gamma + \lambda_i) : f_1 : f_2 : \dots : f_s, \\ U_{i,2} : U_{i,N_b+N_s+1} : U_{i,N_b+N_s+2} : \dots : U_{i,N_b+N_s+N_s} &= (\Gamma + \lambda_i) : f_1 : f_2 : \dots : f_s, \\ U_{i,3} : U_{i,N_b+2N_s+1} : U_{i,N_b+2N_s+2} : \dots : U_{i,N_b+2N_s+N_s} &= (\Gamma + \lambda_i) : f_1 : f_2 : \dots : f_s, \\ &\dots . \end{aligned} \tag{B3}$$

As a result of Eq. (B3), the problem of solving for the $M \times N$ unknowns ($M = 2N_b$) which make up the $\mathbf{U}_P$ submatrix is reduced to solving for $M \times N_b$ matrix elements of U_{ij}, $i \in [1, M]$ and $j \in [1, N_b]$. In other words we can write the $\mathbf{U}_P$ submatrix as

$$\mathbf{U}_P = \begin{bmatrix} U_{1,1} & \dots & U_{1,N_b} & \frac{f_1}{\Gamma+\lambda_1}U_{1,1} & \frac{f_2}{\Gamma+\lambda_1}U_{1,1} & \dots & \frac{f_s}{\Gamma+\lambda_1}U_{1,1} & \frac{f_1}{\Gamma+\lambda_1}U_{1,2} & \frac{f_2}{\Gamma+\lambda_1}U_{1,2} & \dots \\ U_{2,1} & \dots & U_{2,N_b} & \frac{f_1}{\Gamma+\lambda_2}U_{2,1} & \frac{f_2}{\Gamma+\lambda_2}U_{2,1} & \dots & \frac{f_s}{\Gamma+\lambda_2}U_{2,1} & \frac{f_1}{\Gamma+\lambda_2}U_{2,2} & \frac{f_2}{\Gamma+\lambda_2}U_{2,2} & \dots \\ \dots & \dots & \dots & \dots & \dots & \dots & \dots & \dots & \dots & \\ U_{M,1} & \dots & U_{M,N_b} & \frac{f_1}{\Gamma+\lambda_M}U_{M,1} & \frac{f_2}{\Gamma+\lambda_M}U_{M,1} & \dots & \frac{f_s}{\Gamma+\lambda_M}U_{M,1} & \frac{f_1}{\Gamma+\lambda_M}U_{M,2} & \frac{f_2}{\Gamma+\lambda_M}U_{M,2} & \dots \end{bmatrix}. \tag{B4}$$

The determination of $\mathbf{U}_P$ is thus reduced to the solution of a set of $M \times N_b$ ($M = 2N_b$) linear equations:

$$[\mathbf{U}]_{M\times N}\mathbf{h}_{N\times N_b} = [\lambda]_{M\times M}[\mathbf{U}]_{M\times N_b}. \tag{B5}$$

We next discuss the construction of the $\mathbf{U}_{EM}$ submatrix corresponding to the remaining $N - M$ ("Effective-Modes") eigenvalues. $\underline{U}_k$, the (row) eigenvector associated with the $\lambda_k = -\Gamma$ eigenvalue, satisfies the following equation:

$$\underline{U}_k\mathbf{h} = -\Gamma\underline{U}_k. \tag{B6}$$

Using Eqs. (B2) and (B6) the $N - N_b$ matrix elements of $\underline{U}_k$ must satisfy the following N_b equations:

$$\begin{aligned} &U_{k,N_b+1}g^1_{1,1} + U_{k,N_b+2}g^2_{1,1} + \dots + U_{k,N_b+N_s+1}g^1_{2,1} + U_{k,N_b+N_s+2}g^2_{2,1} + \dots + U_{k,N}g^{N_s}_{N_b,1} = 0, \\ &U_{k,N_b+1}g^1_{1,2} + U_{k,N_b+2}g^2_{1,2} + \dots + U_{k,N_b+N_s+1}g^1_{2,2} + U_{k,N_b+N_s+2}g^2_{2,2} + \dots + U_{k,N}g^{N_s}_{N_b,2} = 0, \\ &\dots \\ &U_{k,N_b+1}g^1_{1,N_b} + U_{k,N_b+2}g^2_{1,N_b} + \dots + U_{k,N_b+N_s+1}g^1_{2,N_b} + U_{k,N_b+N_s+2}g^2_{2,N_b} + \dots + U_{k,N}g^{N_s}_{N_b,N_b} = 0. \end{aligned} \tag{B7}$$

We see that $\underline{U}_k$ is underdetermined since we have N_b equations in $N - N_b$ unknowns. For each $\underline{U}_k$ we can therefore choose $N - 2N_b = N - M$ "free" matrix elements at will and then solve for the remaining N_b "essential" matrix elements. We can repeat this procedure to obtain the $(N - M) \times N_b$ matrix elements needed to satisfy Eq. (B7) for all the rows of the $\mathbf{U}_{EM}$ matrix.

In order to guarantee the linear independence of the eigenvectors we choose the "free" matrix elements of $\mathbf{U}_{EM}$ matrix such that the matrix assumes the following form:

$$\mathbf{U}_{EM} = \begin{bmatrix} 0 & \dots & 0 & U_{M+1,N_b+1} & 1 & 0 & \dots & U_{M+1,N_b+N_s+1} & 0 & 0 & \dots & 0 \\ 0 & \dots & 0 & U_{M+2,N_b+1} & 0 & 1 & \dots & U_{M+2,N_b+N_s+1} & 0 & 0 & \dots & 0 \\ \dots & \dots & \dots & \dots & \dots & \dots & \dots & \dots & \dots & \dots & \dots & \dots \\ 0 & \dots & 0 & U_{M+N_s,N_b+1} & 0 & 0 & \dots & U_{M+N_s,N_b+N_s+1} & 1 & 0 & \dots & 0 \\ 0 & \dots & 0 & U_{M+N_s+1,N_b+1} & 0 & 0 & \dots & U_{M+N_s+1,N_b+N_s+1} & 0 & 1 & \dots & 0 \\ \dots & \dots & \dots & \dots & \dots & \dots & \dots & \dots & \dots & \dots & \dots & \dots \\ 0 & \dots & 0 & U_{N,N_b+1} & 0 & 0 & \dots & U_{N,N_b+N_s+1} & 0 & 0 & \dots & 1 \end{bmatrix}. \tag{B8}$$

With this choice, the $U_{k,j}$, $j = N_b + 1, N_b + N_s + 1, N_b + 2N_s + 1, \dots, N_bN_s + 1$, "essential" matrix elements are determined by solving Eq. (B7).

[1] H.-P. Breuer and F. Petruccione, *The Theory of Open Quantum Systems* (Clarendon Press, Oxford, 2006).

[2] J. H. Posthumus and J. F. McCann, *Molecules and Clusters in Intense Laser Fields* (Cambridge University Press, Cambridge, UK, 2001).

[3] A. G. Abrashkevich and M. Shapiro, Phys. Rev. A **50**, 1205 (1994); J. Phys. B: At. Mol. Opt. Phys. **29**, 627 (1996); E. Frishman and M. Shapiro, Phys. Rev. A **54**, 3310 (1996); I. Thanopulos and M. Shapiro, J. Phys. B: At. Mol. Opt. Phys. **41**, 074010 (2008).

[4] H. Stapelfeldt and T. Seideman, Rev. Mod. Phys. **75**, 543 (2003).

[5] M. E. Sukharev, E. Charron, A. Suzor-Weiner, and M. V. Fedorov, Int. J. Quan. Chem. **99**, 452 (2004).

[6] L. J. Frasinski, J. H. Posthumus, J. Plumridge, K. Codling, P. F. Taday, and A. J. Langley, Phys. Rev. Lett. **83**, 3625 (1999).

[7] K. Sändig, H. Figger, and T. W. Hänsch, Phys. Rev. Lett. **85**, 4876 (2000).

[8] A. Assion, T. Baumert, U. Weichmann, and G. Gerber, Phys. Rev. Lett. **86**, 5695 (2001).

[9] I. Ben-Itzhak, P. Q. Wang, J. F. Xia, A. M. Sayler, M. A. Smith, K. D. Carnes, and B. D. Esry, Phys. Rev. Lett. **95**, 073002 (2005).

[10] M. F. Kling *et al.*, Science **312**, 246 (2006).

[11] B. Feuerstein, T. Ergler, A. Rudenko, K. Zrost, C. D. Schroter, R. Moshammer, J. Ullrich, T. Niederhausen, and U. Thumm, Phys. Rev. Lett. **99**, 153002 (2007).
[12] J. J. Hua and B. D. Esry, J. Phys. B **42**, 085601 (2009); Phys. Rev. A **80**, 013413 (2009).
[13] B. M. Garraway, Phys. Rev. A **55**, 4636 (1997); L. Mazzola, S. Maniscalco, J. Piilo, K. A. Suominen, and B. M. Garraway, Phys. Rev. A **80**, 012104 (2009).
[14] I. Thanopulos, P. Brumer, and M. Shapiro, J. Chem. Phys. **133**, 154111 (2010).
[15] R. G. Gordon, J. Chem. Phys. **51**, 14 (1969).
[16] W. Koot, W. J. Van Der Zande, and D. P. De Bruijn, Chem. Phys. **115**, 297 (1987).
[17] V. S. Prabhudesai *et al.*, Phys. Rev. A **81**, 023401 (2010).
[18] A. S. Meijer, Y. Zhang, D. H. Parker, W. J. van der Zande, A. Gijsbertsen, and M. J. J. Vrakking, Phys. Rev. A **76**, 023411 (2007).
[19] X. G. Xu *et al.*, J. Chem. Phys. **126**, 091102 (2007).
[20] A. Han, E. A. Shapiro, and Moshe Shapiro (to be submitted); J. Deiglmayr, A. Grochola, M. Repp, R. Wester, M. Weidemuller, O. Dulieu, P. Pellegrini, and R. Cote, New J. Phys. **11**, 055034 (2009).